APPLIED ORGANOMETALLIC CHEMISTRY
Appl. Organometal. Chem. 2005; **19**: 1002–1009
Published online 20 July 2005 in Wiley InterScience (www.interscience.wiley.com). DOI:10.1002/aoc.948

Synthesis and characterization of zinc bis(*O*-isopropylxanthate) as a single-source chemical vapor deposition precursor for ZnS

Davide Barreca[1]*, Alberto Gasparotto[2], Cinzia Maragno[2], Roberta Seraglia[1], Eugenio Tondello[2], Alfonso Venzo[1], Venkata Krishnan[3] and Helmut Bertagnolli[3]

[1]ISTM-CNR and INSTM, Department of Chemical Sciences, Padova University, Via Marzolo, 1, 35131 Padua, Italy
[2]Department of Chemical Sciences, Padova University and INSTM, Via Marzolo, 1, 35131 Padua, Italy
[3]Institut für Physikalische Chemie, Universität Stuttgart, Pfaffenwalding, 55, 70569 Stuttgart, Germany

Received 24 March 2005; Accepted 9 April 2005

The utilization of single-source molecular precursors in chemical vapor deposition (CVD) experiments requires a deep knowledge of their chemico-physical properties, with particular regard to thermal stability and fragmentation pattern. This study describes the synthesis and characterization of zinc bis(*O*-isopropylxanthate), Zn(*O*-^{i}PrXan)$_2$, [*O*-^{i}PrXan = $(CH_3)_2CHOCS_2$], a single-source precursor for the CVD of zinc(II) sulfide thin films and nanorods. Several analytical methods yielding complementary information (extended X-ray absorption fine structure, Raman, FT-IR, UV–Vis optical absorption, ^{1}H and ^{13}C NMR, thermogravimetric analysis, differential scanning calorimetry as well as mass spectrometry techniques, i.e. electrospray and electron ionization, mass-analyzed ion kinetic energy) are adopted for a comprehensive investigation of purity, structure, thermal behavior and decomposition pathways of the molecule. The most significant results are discussed critically and the properties useful for CVD applications are highlighted. Copyright © 2005 John Wiley & Sons, Ltd.

KEYWORDS: zinc(II) bis(*O*-isopropylxanthate); ZnS; characterization; EXAFS; NMR; mass spectrometry

INTRODUCTION

The use of wide band-gap semiconductor thin films, like zinc(II) sulfide ($E_G = 3.7$ eV),[1–3] in electro- and photoluminescent functional devices[1,4–7] represents a well-established research field both in academic and industrial contexts. As a general rule, the ZnS films produced may possess different chemico-physical properties, depending on the synthetic approach, the precursor nature and processing parameters.[3] Among the various preparative routes, chemical vapor deposition (CVD) has a great potential, thanks to its inherent versatility and to the possibility of operating under *soft* experimental conditions.[8] In this context, the synthesis of semiconducting thin films and nanorods can be conveniently afforded starting from single-source molecular compounds (SSMs), comprising all the desired elements in a unique molecular architecture with a bonding scheme as close as possible to that of the final material.[9,10] The main advantages offered by these compounds with respect to multiple-source reagents have already been reported.[1,9–11] As far as ZnS thin films are concerned, the most common SSMs employed in CVD experiments have been dialkyldithiocarbamates [Zn($S_2CNR'R''$)$_2$; R′, R″ = alkyl groups].[12–15] Nevertheless, their utilization becomes difficult owing to different disadvantages, such as the high decomposition temperatures,[13,14,16] the low growth rates[14,16] and the low transparency of the films obtained.[12,16] Other examples of SSMs include Zn(SOCCH$_3$)TMEDA (TMEDA = *N*,*N*,*N*,*N*-tetramethylethylenediamine), adopted in aerosol-assisted CVD,[17] and Zn(*O*-^{i}PrXan)$_2$ [*O*-^{i}PrXan = $(CH_3)_2CHOCS_2$],[18] used in both thermal and laser-driven CVD. In the latter case, no detailed results concerning the precursor decomposition pathways under thermal CVD conditions and the resulting ZnS film characteristics are available.

In recent years our research group has focused on the synthesis and characterization of metal sulfide thin

*Correspondence to: Davide Barreca, ISTM-CNR and INSTM, Department of Chemical Sciences, Padova University, Via Marzolo, 1, 35131 Padua, Italy.
E-mail: barreca@chin.unipd.it

films (ZnS, CdS, $Zn_xCd_{1-x}S$) starting from M(II) bis(*O*-alkylxanthate) compounds (M = Zn, Cd).[7,11,19–22] Following our recent work on cadmium(II) bis(*O*-alkylxanthate) precursors,[23] we have subsequently focused our attention on Zn(*O*-RXan)$_2$ compounds [*O*-RXan = $CH_3CH_2OCS_2$ (*O*-EtXan) or $(CH_3)_2CHOCS_2$ (*O*-^{i}PrXan)] and, in particular, to the use of Zn(*O*-^{i}PrXan)$_2$ as an SSM for the CVD of ZnS-based films. Despite Zn(*O*-^{i}PrXan)$_2$ has already been used in CVD experiments,[18] previous studies have mainly been focused on its structural characteristics,[24,25] whereas the investigation of its decomposition pathways has not been completely exhaustive. In this context, this paper is devoted to a detailed characterization of Zn(*O*-^{i}PrXan)$_2$, with the final aim of elucidating its relevant properties as an SSM for the CVD of zinc(II) sulfide. Similar to our recent paper on cadmium(II) bis(*O*-alkylxanthate) compounds,[23] we have adopted many analytical techniques aimed at gaining as much information as possible on the behavior of zinc(II) bis(*O*-isopropylxanthate) in the solid state and in solution, investigating thus its relevant structure–properties interrelations and turning finally to its thermal behavior and fragmentation pattern.

RESULTS AND DISCUSSION

The Zn(*O*-^{i}PrXan)$_2$ triclinic structure[24] comprises isolated centrosymmetric 16-membered rings, each containing four zinc atoms. The coordination around each zinc can be considered as distorted tetrahedral with four covalent Zn–S bonds.[25] Two sulfur atoms around each zinc center belong to a chelating xanthate group, and the remaining positions are bound to two different bidentate $(CH_3)_2CHOCS_2$ ligands.[11,25] These tetramers are packed three-dimensionally via van der Waals interactions between sulfur–methyl and methyl–methyl groups.[24]

In order to attain a deeper insight on the coordination geometry of zinc bis(*O*-isopropylxanthate), a preliminary solid-state characterization was performed by extended X-ray absorption fine structure (EXAFS), Raman and FT-IR spectroscopies.

The results of EXAFS analysis are displayed in Fig. 1 and the corresponding structural parameters are summarized in Table 1. The experimental k^3-weighted $\chi(k)$ function indicated the presence of four sulfur backscatterers at a distance of about 2.34 Å, with no appreciable contribution from other shells. The value obtained is very close to those previously reported for Zn(*O*-^{i}PrXan)$_2$,[24] with a Debye–Waller factor equal to 0.081 Å. Moreover, the Zn–S distance obtained and the coordination number were in good agreement with those of crystalline zinc sulfide,[26] indicating that the SSM precursor investigated possesses a core structure very similar to the 'building blocks' of ZnS.

The Raman and FT-IR spectra of Zn(*O*-^{i}PrXan)$_2$ are displayed in Fig. 2 and Fig. 3 respectively; the band assignments, based on literature data,[27–33] are summarized in Table 2. The Zn–S stretching vibrations were determined at 319 and 405 cm^{-1}. The CS_2 in-phase stretching at 650 cm^{-1} was clearly evident in the Raman analysis (Fig. 2). In the FT-IR spectrum (Fig. 3), the prominent signals at 1030 and 1090 cm^{-1} were attributed to CS_2 and CCC out-of-phase stretching, in good agreement with Raman results. The intense absorptions in the range 1190–1250 cm^{-1} were assigned to COC out-of-phase stretching.

Table 1. Structural parameters of Zn(*O*-^{i}PrXan)$_2$ obtained by EXAFS analysis

Absorber–backscatterer distance	Zn–S
Coordination number *N*	4.2 ± 0.4
Interatomic distance *r* (Å)	2.34 ± 0.02
Debye–Waller factor σ (Å)	0.081 ± 0.008
Threshold energy shift ΔE_0 (eV)	15.30
k-range (Å^{-1})	3.0–15.0
Fit index	21.92

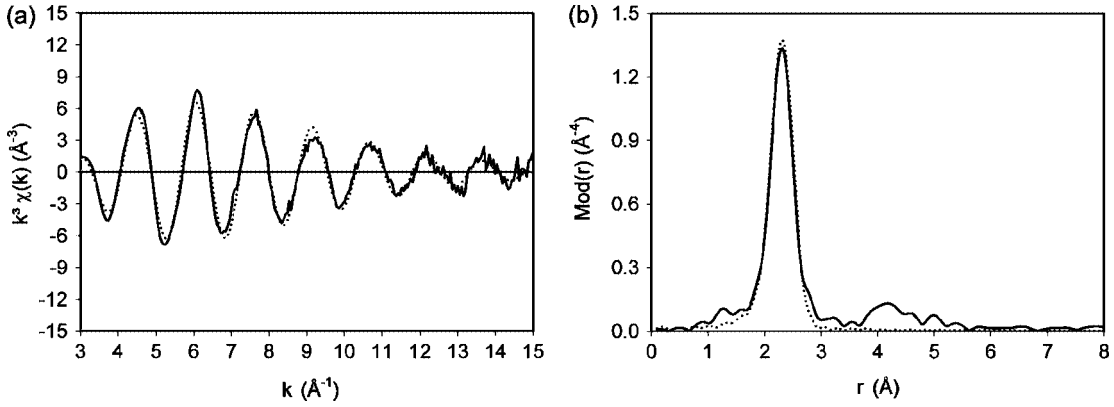

Figure 1. Experimental (solid line) and theoretical (dotted line) EXAFS functions (a) and their Fourier transforms (b) for Zn(*O*-^{i}PrXan)$_2$ measured at the zinc K-edge.

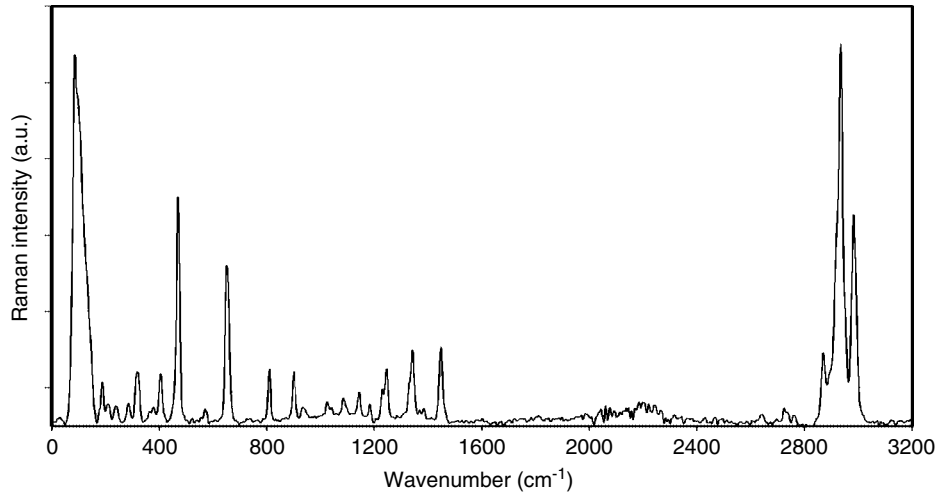

Figure 2. Raman spectrum of Zn(*O*-^{i}PrXan)$_2$.

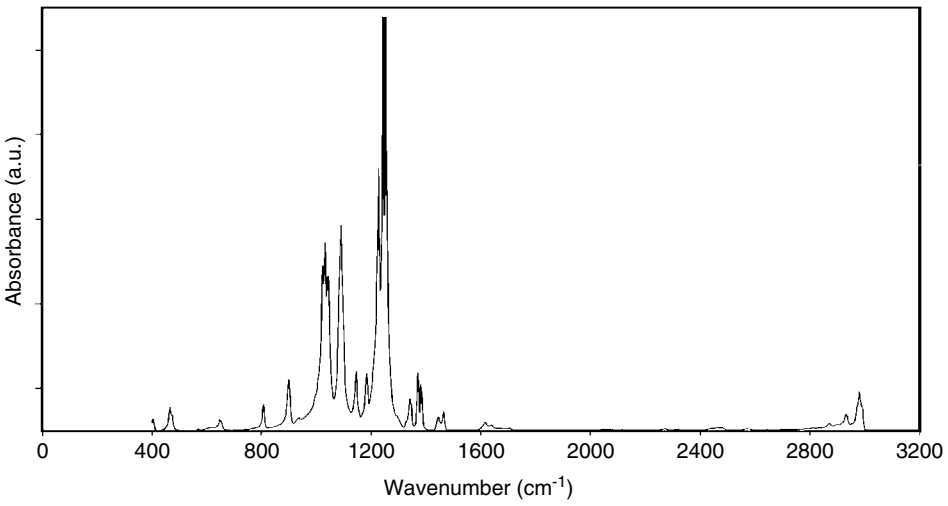

Figure 3. FT-IR spectrum of Zn(*O*-^{i}PrXan)$_2$.

Other significant Raman bands (Fig. 2) were located as follows: 87 cm^{-1}, lattice vibrations; 470 cm^{-1}, COC and CCC in-phase bending modes; 2940 and 2990 cm^{-1}, CH_3 out-of-phase stretching vibrations.

Subsequently, UV–Vis optical absorption and NMR spectroscopy were employed for a characterization of Zn(*O*-^{i}PrXan)$_2$ in solution.

The optical absorption spectrum of zinc bis(*O*-isopropylxanthate) in ethanol solution (Fig. 4) was characterized by a complete transparency in the visible range and by the occurrence of two intense bands in the UV region, located at $\lambda = 230$ and 298 nm. The close resemblance of the spectrum with those recorded for cadmium bis(*O*-alkylxanthate) compounds[23] allowed us to rule out unambiguously any appreciable contribution from the metal centers to the absorption signals detected. In particular, the bands at $\lambda = 230$ nm and 298 nm were attributed to $n \rightarrow \sigma^*$ and $n \rightarrow \pi^*$ transitions of the xanthate ligand respectively, while the weak shoulder located at $\lambda = 315$ nm was assigned to $\pi \rightarrow \pi^*$ ones.[23,34,35]

NMR spectra of 0.1 M Zn(*O*-^{i}PrXan)$_2$ in $(CD_3)_2SO$-d_6 ($\varepsilon = 32$) indicated that, in solution, all the xanthate units were equivalent. In particular, the ^{1}H signals of the methyl (CH_3) and methine (C*H*) protons were observed at δ 1.243 and 5.276 (doublet and septet) respectively. The corresponding ^{13}C resonances appeared at δ 21.64 and 78.26, in addition to the signal of the dithiocarbonyl carbon at δ 228.56.

Further NMR measurements were performed in $CDCl_3$ ($\varepsilon = 4.8$). Despite the lower solubility of zinc bis(*O*-isopropylxanthate) in this solvent, the NMR spectrum was found to be very similar to that observed in the previous case [^{1}H NMR: δ 1.452 (CH_3), δ 5.340 (C*H*). ^{13}C NMR: δ 21.50 (CH_3), δ 83.03 (*C*H), δ 228.63 (CS_2)], indicating a negligible solvent influence on the precursor behavior in solution.

Table 2. Selected features and corresponding assignments in the vibrational spectra of Zn(*O*-^{i}PrXan)$_2$

Raman frequency (cm^{-1})	IR frequency (cm^{-1})	Assignment
87		Lattice vibrations
188		CS_2 rocking
319		Zn–S stretching vibrations; SCS, CCC in-phase bending
405		Zn–S stretching vibrations; CCC, SCS out-of-phase bending
469	466	COC, CCC in-phase bending
572		OCS_2 wagging
652	648	CS_2 in-phase stretching
809	809	OCC_2 in-phase stretching
901	899	CH_3 out-of-phase rocking perpendicular to *O*-C(H)
935		CH_3 out-of-phase rocking parallel to *O*-C(H)
1030	1022, 1031	CS_2 out-of-phase stretching
1090	1090	CCC out-of-phase stretching
1150	1145	C–C, (S)C–O stretching
1191, 1235, 1250	1183, 1245, 1255	COC out-of-phase stretching
1350	1343	CH wagging parallel to *O*-C(H)
1390	1371, 1382	CH_3 in-phase deformation
1450	1466	CH_3 out-of-phase deformation
2870	2872	CH_3 in-phase stretching
2940	2931	CH_3 out-of-phase stretching
2988	2979	CH_3 out-of-phase stretching

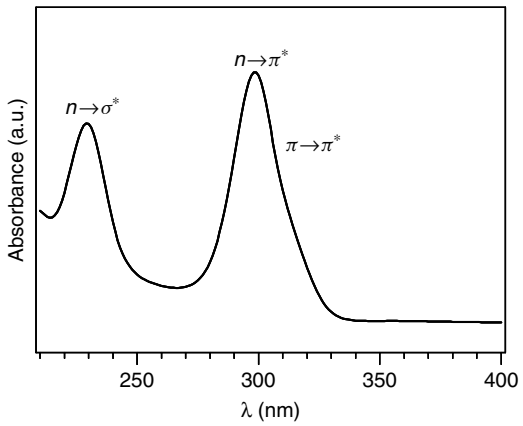

Figure 4. Optical absorption spectra of Zn(*O*-^{i}PrXan)$_2$ recorded on 10^{-4} M ethanolic solutions.

Finally, attention was devoted to the relevant properties of Zn(*O*-^{i}PrXan)$_2$ for application as an SSM in the CVD of zinc(II) sulfide, focusing in particular on its thermal decomposition and fragmentation behavior.

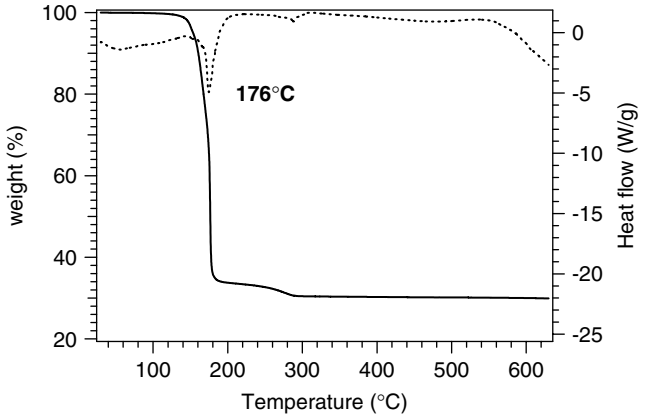

Figure 5. TGA (solid line) and DSC (dotted line) traces of Zn(*O*-^{i}PrXan)$_2$.

Similar to Cd(*O*-^{i}PrXan)$_2$,[23] thermal analyses on Zn(*O*-^{i}PrXan)$_2$ were performed under nitrogen flow in order to avoid undesired oxidations. The thermogravimetric analysis (TGA) curve obtained (Fig. 5) closely resembled the one reported for the homologous cadmium precursor.[23] The compound remained stable up to 120 °C and subsequently underwent a remarkable weight loss, associated with powder vaporization, as confirmed by the endothermic signal at $T = 176$ °C in the differential scanning calorimetry (DSC) curve. At higher temperatures (200–300 °C) a further weight loss took place, leading to a constant mass of 29.9%, in very good agreement with the value expected for the formation of ZnS (theoretical: 29.9%). This result, similar to that obtained for Zn(*O*-EtXan)$_2$,[7] pointed to the suitability of Zn(*O*-^{i}PrXan)$_2$ as an SSM for the CVD of zinc(II) sulfide under an inert atmosphere.

Further information on the fragmentation pathways of zinc bis(*O*-isopropylxanthate) were gained by mass spectrometry (MS) analyses, and, in particular, by the use of both 'soft' and 'hard' ionization techniques, namely electrospray ionization (ESI)[36] and electron ionization (EI) respectively.

The ESI spectra of Zn(*O*-^{i}PrXan)$_2$ were recorded in both positive- and negative-ion modes. The mass spectrometric behavior of Zn(*O*-^{i}PrXan)$_2$ under ESI conditions strongly resembled that obtained for Cd(*O*-^{i}PrXan)$_2$.[23] In the negative-ion mode (Fig. 6a), the ESI spectrum was characterized by the presence of ions corresponding to Zn(*O*-^{i}PrXan)$_3^-$ at m/z 469 (Fig. 6a), displaying the typical pattern due to the four zinc isotopes, and ions originating from successive losses of CS_2 (m/z 393, 317 and 242). The signal at m/z 135 was due to [*O*-^{i}PrXan]$^-$ ions. MS^n experiments carried out on the *pseudo*molecular ion at m/z 469 confirmed that the most favored decomposition pathway involved successive CS_2 losses.

In the positive-ion mode (Fig. 6b), the ESI mass spectrum was dominated by the presence of an intense peak at m/z 537, corresponding to a dinuclear ionic cluster of formula

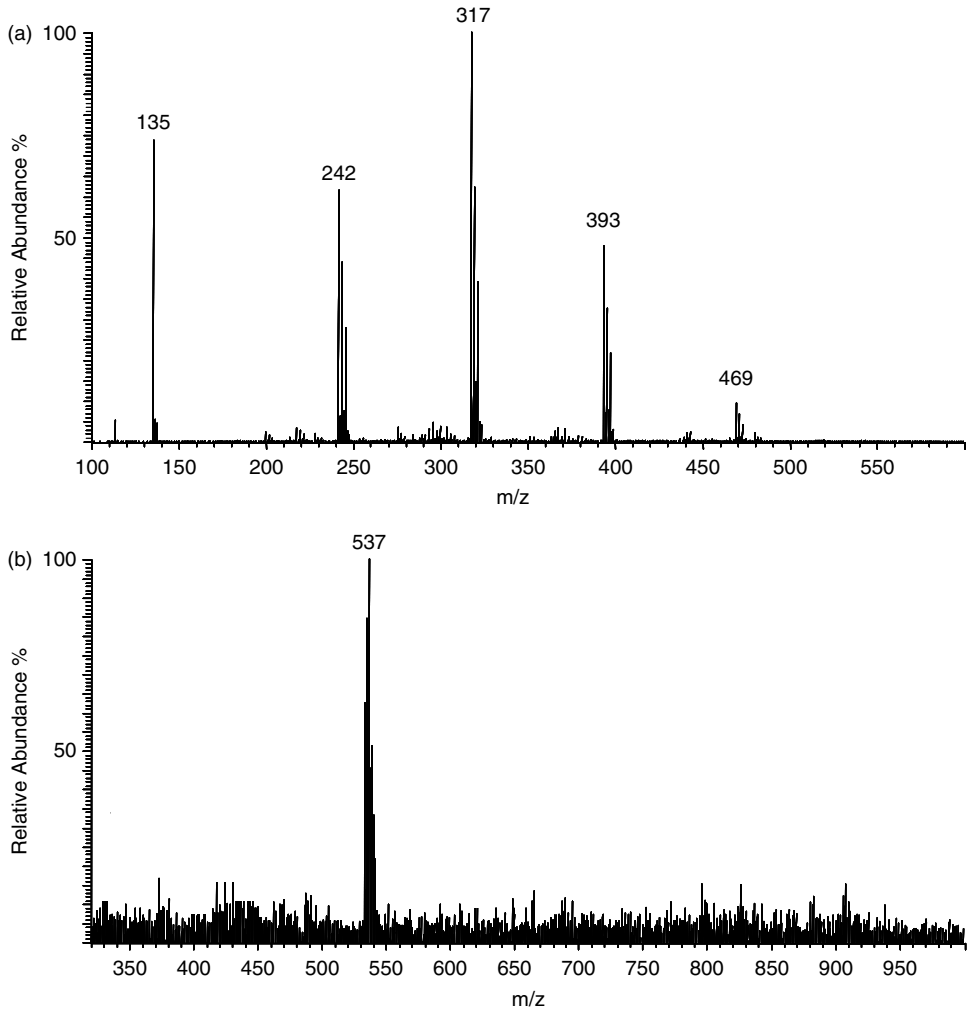

Figure 6. ESI mass spectra of chloroform solution of $Zn(O\text{-}^{i}PrXan)_2$ recorded in (a) negative-ion mode and (b) positive-ion mode.

$Zn_2(O\text{-}^{i}PrXan)_3^+$. This attribution could be unambiguously confirmed by the good agreement of theoretical and experimental isotopic clusters.

As in the case of cadmium derivatives,[23] under ESI experimental conditions the Zn–S bond seemed weaker than the C–S bond, thus favoring the molecular decomposition process involving subsequent CS_2 losses.

In order to obtain a deeper insight into the $Zn(O\text{-}^{i}PrXan)_2$ behavior in the gas phase, i.e. under conditions more similar to those of CVD processes, EI measurements were carried out. The resulting spectrum (Fig. 7a) was characterized by the presence of $M^{+\bullet}$ ions, as a cluster, at m/z 334. Sequential losses of C_3H_6 led to the formation of ions at m/z 292 and 250. The ions at m/z 189 could originate from species at m/z 250 through $[CHOS]^{\bullet}$ loss, and the peak at m/z 157 corresponded to $[ZnS_2COH]^+$. The peaks at m/z 128, 96 and 60 were assigned to $ZnS_2^{+\bullet}$, $ZnS^{+\bullet}$ and $[^{i}PrOH]^{+\bullet}$ species respectively. At variance with the results obtained for $Cd(O\text{-}^{i}PrXan)_2$,[23] an intense signal at m/z 76 was detected and attributed to $CS_2^{+\bullet}$ ions.

Mass-analyzed ion kinetic energy (MIKE) experiments[37] carried out on the $M^{+\bullet}$ ions of $Zn(O\text{-}^{i}PrXan)_2$ led to the spectrum reported in Fig. 7b. The most favored decomposition pathway was due to the formation of $ZnS^{+\bullet}$ at m/z 96, whereas the signal at m/z 64 corresponded to $Zn^{+\bullet}$ ions. The loss of a ligand from the $M^{+\bullet}$ ions led to the ionic species at m/z 199, and the signal at m/z 157 was attributed to ZnS_2COH^+. A minor peak at m/z 292 was detected and attributed to the loss of C_3H_6 from the parent ion.

As in the case of mass spectrometric analysis of $Cd(O\text{-}^{i}PrXan)_2$,[23] ESI conditions seemed to induce precursor decomposition, due to and/or reducing processes occurring during the ionization to interaction with solvent, which made the Zn–S bond weaker than in the solid or gas phase. In fact, the preparation of ZnS thin films from $Zn(O\text{-}^{i}PrXan)_2$ was successfully performed under nitrogen flow at a substrate temperature between 200 and 500 °C.[11,20,22] These phenomena point to the stability of Zn–S moieties in the gas phase, thus indicating the suitability of $Zn(O\text{-}^{i}PrXan)_2$ as a single-source CVD precursor for zinc(II) sulfide.

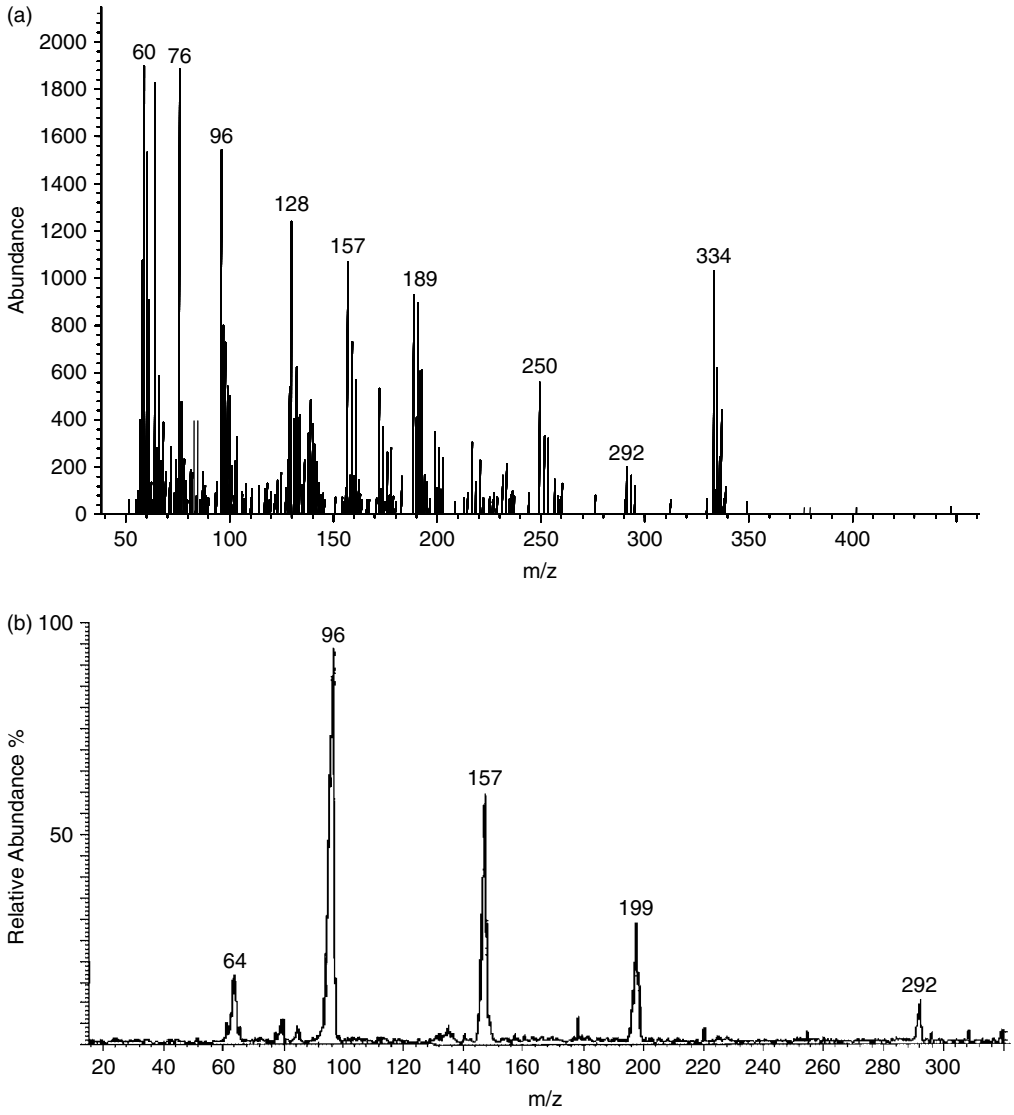

Figure 7. (a) EI mass spectrum of Zn(*O*-^{i}PrXan)$_2$ and (b) MIKE spectrum of the corresponding $M^{+\bullet}$ ions at *m/z* 334.

CONCLUSIONS

This paper has focused on the synthesis and chemical characterization of zinc bis(*O*-isopropylxanthate), an SSM precursor for the CVD of ZnS thin films and nanorods. The compound was synthesized and subjected to a multi-technique characterization, in order to obtain complementary data regarding its behavior in the solid state (EXAFS, FT-IR, Raman) and in solution (UV–Vis, NMR). Finally, the chemical reactivity of Zn(*O*-^{i}PrXan)$_2$, with particular attention to relevant properties for CVD applications, was investigated by thermal analysis (TGA, DSC) and MS (ESI, EI, MIKE) experiments. The latter analyses showed the presence of a *solvent effect*, leading to a weakening of Zn–S bonds with respect to C–S bonds when such complexes are analyzed by ESI. In fact, subsequent losses of CS_2 observed in the ESI spectra were negligible under EI conditions.

Besides obtaining a fingerprint identification of the different chemical moieties in Zn(*O*-^{i}PrXan)$_2$, the results reported here reveal that such a compound possesses a core architecture very similar to that of crystalline ZnS. This result, together with the clean decomposition and fragmentation pattern and the appreciable volatility, constitutes a significant advantage for the use of zinc bis(*O*-isopropylxanthate) as an SSM precursor in the CVD of ZnS thin films and nanorods.[11,21,22]

EXPERIMENTAL

Synthesis

Zn(*O*-^{i}PrXan)$_2$ was prepared according to the literature.[38] An aqueous solution of potassium (*O*-isopropylxanthate) [K(*O*-^{i}PrXan)], prepared as reported previously[23] (15.2 mmol

in 22 cm^3 H_2O), was added dropwise to a solution of $Zn(NO_3)_2$ (Alpha Aesar®, 7.6 mmol in 36 cm^3 H_2O), resulting in the precipitation of a white solid. After 1 h stirring, vacuum-filtering and drying allowed the recovery of a white $Zn(O\text{-}^iPrXan)_2$ powder (yield ~85%). Light exposure during preparation and storage must be avoided, since the resulting compound is slightly photosensitive.

Elemental analyses

Found: C, 29.1%; H, 4.7%; S, 38.1%. Calculated: C, 28.6%; H, 4.7%; S, 38.1%.

Characterization

The EXAFS measurements on zinc bis(*O*-isopropylxanthate) was performed at the zinc K-edge at 9659 eV at the beamline X1.1, at the Hamburg Synchrotron Radiation Laboratory (HASYLAB) at DESY, Hamburg, with an Si(111) double crystal monochromator under ambient conditions. The positron energy was 4.45 GeV and the beam current was about 120 mA. Data were collected in transmission mode with ion chambers filled with nitrogen. Energy calibration was monitored with a 20 μm thick zinc metal foil. The sample in the solid state was embedded in a polyethylene matrix and pressed into a pellet. The concentration of the solid sample was adjusted to yield an extinction of 1.5. The data analysis was performed as described elsewhere.[23] In the fitting procedure, the parameters (the coordination number, interatomic distance, Debye–Waller factor and energy zero value) were determined by iteration.

A Bruker RFS 100/S FT spectrometer (spectral resolution 4 cm^{-1}) with a Nd:YAG laser ($\lambda = 1064$ nm; power = 150 mW) was used for the Raman measurements. The scattered light was collected with a high-sensitivity germanium diode. To obtain an average measurement, 1024 scans were accumulated.

FT-IR spectra were recorded on KBr-containing pellets under ambient conditions by means of a Bruker IFS 66v/S FT-IR spectrometer with a DLATGS detector in absorption mode, with a spectral resolution of 2 cm^{-1}.

Optical absorption measurements were performed by a Cary 5E (Varian) UV–Vis–NIR dual-beam spectrophotometer with a spectral bandwidth of 1 nm. Measurements were carried out in quartz cuvettes (optical path = 0.5 mm).

^1H and ^{13}C NMR spectra were recorded on $CDCl_3$ and $(CD_3)_2SO$ solutions at 298 K on a Bruker Avance 400 NMR spectrometer operating at $\nu_o = 400.13$ MHz and 100.61 MHz respectively. The chemical shift values δ (ppm) were reported against internal Me_4Si.

Thermal analyses were performed by an SDT 2960 apparatus from TA Instruments (New Castle, USA), which allows simultaneous DSC–TGA measurements to be performed. The traces were recorded under nitrogen flow with a heating rate of 10 °C min^{-1}.

The ESI mass spectra were obtained using an LCQ instrument (Finnigan, Palo Alto, CA, USA), operating in both positive- and negative-ion modes. The entrance capillary temperature was 200 °C and the capillary voltage was kept at ±5 kV. Solutions (10^{-6} M) were introduced by direct infusion using a syringe pump at a flow rate of 8 μl min^{-1}. The helium pressure inside the trap was kept constant. The pressure in the absence of the nitrogen stream was 2.8×10^{-5} Torr, as measured by an ion gauge.

EI measurements were performed on a VG AutoSpec mass spectrometer (Micromass, Manchester, UK). The working conditions were as follows: 70 eV, 200 μA, ion source temperature 200 °C. Metastable ionic species were detected by MIKE spectrometry.

Acknowledgements

This work was partially funded by Consorzio OPTEL-PNR, Art. 10, legge 46/1982. Thanks are also due to Padova University and CNR for financial support. Professor T.R. Spalding (University College, Cork, Ireland) and Dr R. Saini (Padova University, Padova, Italy) are acknowledged for assistance in precursor synthesis and thermal analyses respectively. Special thanks are also due to Ms J. Hollmann for her help in FT-IR measurements. HASYLAB at DESY, Hamburg, is gratefully acknowledged for the provision of synchrotron radiation for EXAFS measurements.

REFERENCES

1. O'Brien P, Haggata S. *Adv. Mater. Opt. Electron.* 1995; **5**: 117.
2. Fernández M, Prete P, Lovergine N, Mancini AM, Cingolani R, Vasanelli L, Perrone MR. *Phys. Rev. B* 1997; **55**: 7660.
3. Su B, Choy KL. *J. Mater. Chem.* 2000; **10**: 949.
4. Piquette EC, Bandić ZZ, McCaldin JO, McGill TC. *J. Vac. Sci. Technol. B* 1997; **15**: 1148.
5. Thiandoume C, Ka O, Lusson A, Gorochov O. *J. Cryst. Growth* 1999; **197**: 805.
6. Wei M, Choy KL. *Chem. Vap. Depos.* 2002; **8**: 15.
7. Barreca D, Tondello E, Lydon D, Spalding TR, Fabrizio M. *Chem. Vap. Depos.* 2003; **9**: 93 and references cited therein.
8. Prete P, Lovergine N, Cannoletta D, Mancini AM, Mele G, Vasapollo G. *J. Appl. Phys.* 1998; **84**: 6460.
9. Maury F. *Chem. Vap. Depos.* 1996; **2**: 113.
10. Gleizes AN. *Chem. Vap. Depos.* 2000; **6**: 155.
11. Barreca D, Gasparotto A, Maragno C, Tondello E. *J. Electrochem. Soc.* 2004; **151**: G428 and references cited therein.
12. Frigo DM, Khan OFZ, O'Brien P. *J. Cryst. Growth* 1989; **96**: 989.
13. Bessergenev VG, Ivanova EN, Kovalevskaya YA, Vasilieva IG, Varand VL, Zemskova SM, Larinov SV, Kolesov BA, Ayupov BM, Logvinenko VA. *Mater. Res. Bull.* 1997; **32**: 1403.
14. O'Brien P, Walsh JR, Watson IM, Motevalli M, Henriksen L. *J. Chem. Soc. Dalton Trans.* 1996; **12**: 2491.
15. Zavyalova LV, Savin AK, Svechnikov GS. *Display* 1997; **18**: 73.
16. Motevalli M, O'Brien P, Walsh JR, Watson IM. *Polyhedron* 1996; **15**: 2801.
17. Nyman M, Hampden-Smith MJ, Duesler EN. *Chem. Vap. Depos.* 1996; **2**: 171.
18. Cheon J, Talaga DS, Zink JI. *J. Am. Chem. Soc.* 1997; **119**: 163.
19. Barreca D, Gasparotto A, Maragno C, Tondello E. *Surf. Sci. Spectra* 2002; **9**: 46.
20. Barreca D, Gasparotto A, Maragno C, Tondello E, Spalding TR. *Surf. Sci. Spectra* 2002; **9**: 54.
21. Armelao L, Barreca D, Bottaro G, Gasparotto A, Maragno C, Sada C, Spalding TR, Tondello E. *Electrochem. Soc. Proc.* 2003; **8**: 1104.

22. Barreca D, Gasparotto A, Maragno C, Tondello E, Sada C. *Chem. Vap. Depos.* 2004; **10**: 229.
23. Barreca D, Gasparotto A, Maragno C, Seraglia R, Tondello E, Venzo A, Krishnan V, Bertagnolli H. *Appl. Organometal. Chem.* 2005; **19**: 59.
24. Ito T. *Acta Crystallogr. Sect. B* 1972; **28**: 1697.
25. Cox MJ, Tiekink ERT. *Rev. Inorg. Chem.* 1997; **17**: 1.
26. Kisi EH, Elcombe MM. *Acta Crystallogr. Sect. C* 1989; **45**: 1867.
27. Colthup NB, Powell LP. *Spectrochim. Acta Part A* 1987; **43**: 317.
28. Weidlein J, Müller U, Dehnicke K. *Schwingungsspektroskopie*, 2nd edn. Georg Thieme Verlag: Stuttgart, 1988.
29. Siiman O, Titus DD, Cowman CD, Fresco J, Gray HB. *J. Am. Chem. Soc.* 1974; **96**: 2353.
30. Little LH, Poling GW, Leja J. *Can. J. Chem.* 1961; **39**: 745.
31. Bowmaker GA, Whiting R, Ainscough EW, Brodie AM. *Aust. J. Chem.* 1975; **28**: 1431.
32. Mattes R, Pauleickhoff G. *Spectrochim. Acta Part A* 1974; **30**: 379.
33. Hunt MR, Kruger AG, Smith L, Winter G. *Aust. J. Chem.* 1971; **24**: 53.
34. Shankaranarayana ML, Patel CC. *Acta Chem. Scand.* 1965; **19**: 1113.
35. Kolninov OV, Vozzhennikov VM, Zvonkova ZV, Rukhadze EG, Glushkova VP, Terent'ev AP. *Dokl. Akad. Nauk SSSR* 1968; **181**: 1420.
36. Fenn B, Mann M, Meng CK, Wong SF, Whitehouse CM. *Science* 1989; **246**: 64.
37. Cooks RG, Beynon JH, Caprioli RM, Lester GR. *Metastable Ions*. Elsevier: Amsterdam, 1973.
38. Rao SR. *Xanthate and Related Compounds*. Marcel Dekker: New York, 1971.